

Face recognition using 3D surface-extracted descriptors

Ana Belén Moreno, Ángel Sánchez, José Fco. Vélez and Fco. Javier Díaz
Escuela Superior de CC. Experimentales e Ingeniería, Universidad Rey Juan Carlos,
Campus de Móstoles, C/ Tulipán s/n; 28933 Móstoles; Spain
{a.b.moreno, an.sanchez, j.velez, f.j.diaz}@escet.urjc.es

Abstract

The discriminating power of three dimensional (3D) descriptors extracted from 3D human face surfaces is analyzed. An automatic face recognition system using different subsets of the descriptor set has been implemented and tested. We used 420 3D-facial meshes belonging to 60 individuals, including views presenting light rotations and facial expressions, for the experiments. An HK segmentation (based in the signs of the mean and Gaussian curvatures) for isolating regions of pronounced curvature has been performed. Eighty six descriptors have been obtained from the segmented regions. The thirty five more discriminating ones in frontal views provide 78% of recognition success rate when best match is selected, and a 92% of recognition success is obtained when the five best matches are selected.

Keywords: Face recognition, 3D vision, 3D descriptors, range image recognition.

1 Introduction

A biometric system is a pattern recognition system that determines the authenticity of an individual using some physical or behavior features (fingerprints, face images, signature, voice and so on) [13][11]. The social demand of fraud control in many situations, including geographical movement, in which it is necessary to establish personal authentication contributes to the need for increased research in such systems [10]. A perfect identification is not actually possible, but the integration of more than one personal feature in the biometric system allows to increase the identification rate (i.e. using face and voice) and to deal with the problem when an individual lacks a particular feature. Among the different biometric techniques those using face images, voice and way of walking are the less intrusive ones; in general, the use of face images requires little user collaboration and it is the common technique used by humans to identify persons [11]. Excellent results have been obtained when 2D intensity images are used under uniform acquisition conditions [12][13]. That is why the research effort in this field is actually more oriented to the independence of these conditions (i.e. robustness under illumination changes, geometrical transforms, facial expressions, make-up, hair, and so on).

In the last few years, the interest in automatic face recognition systems 3D model-based has increased [6][7][5][1][15][3]. One common technique on 3D object recognition is based on the correspondence among scene points and model points in order to perform the recognition and to determinate the object pose and location [2]. Among the 3D free-form object descriptors to represent objects is the curvature of the local surface evaluated in each point, which is characterized by the directions in which the normal of the surface changes more and less quickly [8]. In Hallinan et al, a set of twelve 3D feature extracted from segmented regions using curvature properties of the surface were experimented for face recognition using a database of 8 individual and 3 images per individual obtaining 95,5% of recognition rate providing a previous 100% of correct feature extraction [4]. Our work is centered on the searching, discriminating power analysis and selection of specific descriptors extractable from face range images. A set of eighty six features have been employed, using a database of 420 3D range images, 7 images per each one of a set of 60 individuals, 3 of them presenting facial expressions and two of them presenting light rotations. These images consist in 3D polygonal meshes without color information. Database acquisition, segmentation (using the HK algorithm based on the signs of the median and Gaussian curvatures), curvature threshold (to isolate regions of pronounced curvature), feature extraction, analysis of the discriminating power in order to achieve a feature selection and recognition experiments have been the tasks in the implementation of our face recognition system. We obtained 78%, 84%, 86% and 92% of recognition rates when one, two, three and five best matches were respectively selected (using frontal views containing whole features correctly extracted) and corresponding recognition rates 71%, 67%, 80%, 83,33% and 91,67% were obtained when all of the frontal

images were used as test set (including those in which not all regions and consequently features could be located). In order to improve these results, we have determined some future work lines given at the end of this paper. On the other hand, the importance of using an extensive face database and the analysis of discriminating capacity of the many extracted 3D descriptors ensures the accuracy of obtained results and the application of proposed 3D face recognition approach.

Section 2 describes the database used to perform our experiments. Section 3 describes our face recognition system. Section 4 describes the segmented regions and lines, shows the employed segmentation method and gives the obtained results of this stage. Section 5 describes the extracted facial features from the segmented regions and lines. Section 6 analyzes the discriminating capacity of the features providing a selected subset of them containing the more discriminating features that will be employed in our experiments. Section 7 describes the face recognition experiments and their recognition rates. Finally, section 8 gives the conclusions and the future work.

2 Database description

A set of 420 3D facial surfaces has been acquired under variable illumination conditions using a 3D digitizer. The background is empty because the digitizer does not sample the objects (i.e. the wall) placed far from the focused faces. The database consists of 7 different frontal captures for each one of 60 person of white race and aged between 18 and 55. Each set of 7 samples of an individual contains: one facial image in which individual is looking down ($+35^\circ$ x rotation approximately), one facial image in which individual is looking up (-35° x rotation approximately), and five frontal views three of them presenting facial expressions (a random gesture, laugh and smile respectively). Many times dark parts of the face (like eyelids as we can appreciate in the face example of Figure 2) do not reflect light and consequently they are not scanned, obtaining in these cases incomplete facial surfaces (register of different views was not performed, instead of it only one shot images were obtained). Neck, ears and hair were removed manually when they were present. Most of the individuals (99%) had not bear neither glasses. Fig. 1 shows seven 2D images of the same person corresponding to the views the database contains for each individual. This figure also shows one mesh corresponding to one of them as was acquired by the 3D digitizer [9].

Facial surfaces are represented by meshes provided by the range laser sensor. Thousand of points which approximate the surface of each sampled face, and the connections of these points, form a mesh representing the scanned face. Cells of the mesh have four nodes. The grid provides an easy way of establishing two “orthogonal” directions (horizontal and vertical) along which it is possible going from one node to its neighbour in the mesh. The average points per face in whole database is 2,186. A pre-processing stage for removing noise and smoothing were carried out over all the 3D facial meshes using median and Gaussian filters, respectively.



Fig. 1. Views of an individual whose corresponding 3D facial surface meshes belong to the database, and a 3D facial mesh example.

3 Face recognition system description

The proposed recognition system performs the following classical stages: segmentation of regions and lines of interest, feature extraction from the segmented regions and lines, classification using feature vector matching according to the minimum Euclidean distance classifier. When an unknown 3D facial mesh (test face) is going to be recognised by the system, these stages are applied to it. These stages also have been applied to the known faces forming the system database (training set) during the recognition system creation. A previous feature selection to obtain the maximum discriminating power was performed being the resulting features, the components of the feature vectors that represent the faces in our face recognition system. Following sections explain these stages in detail.

4 Segmentation stage

The HK segmentation method [14] performs a point classification in range images according to the local shape around each point. This allows the labelling of the different surface patches in a 3D facial mesh

according to their shape, based on differential geometry. The 3D surface regions are characterised as concave elliptical, convex elliptical, hyperbolic, concave cylindrical, convex cylindrical or planar. Signs of the median (H) and Gaussian (K) curvatures are considered to achieve these point classification. The first step is to compute both median and Gaussian curvatures in each point, using the following formulae:

$$H = \frac{(1 + I_x^2)I_{yy} - 2I_xI_yI_{xy} + (1 + I_y^2)I_{xx}}{2(1 + I_x^2 + I_y^2)^{3/2}} \quad (1)$$

$$K = \frac{I_{xx}I_{yy} - I_{xy}^2}{(1 + I_x^2 + I_y^2)^2} \quad (2)$$

where I_x, I_y , are the first derivative of the surface along x and y directions respectively, and I_{xy}, I_{xx}, I_{yy} represent the corresponding second derivatives. Signs of the H and K curvatures of each point for an example face are represented in the Figures 2(a) and (b), respectively. Brighter points are those in which the corresponding curvature value is positive, and darker ones are those with negative curvature values. Curvatures can not be evaluated in points of the surface contour, where it is no possible computing the second derivative. Figure 2(c) shows the resulting point classification based on sign of curvatures. Three kind of points are obtained: darkest ones are hyperbolic points ($K < 0$), intermediate grey level ones are elliptical convex points ($H < 0$ and $K > 0$), and brightest ones are elliptic concave points ($H > 0$ and $K > 0$). Cylindrical points (if $K = 0$ and $H < 0$ then the point is convex cylindrical; and if $H > 0$, then it is concave cylindrical) and planar points ($H = 0$ and $K = 0$) do not appear since it would be difficult to obtain exactly zero curvature values.

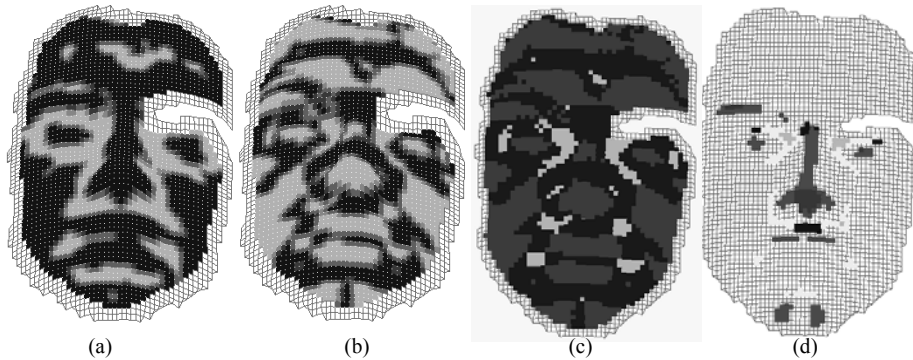


Fig.2. Sign of (a) median and (b) Gaussian curvatures; (c) point HK classification and (d) HK classification after curvature thresholding.

In order to isolate regions of high curvature avoiding points in which low curvature were obtained, different curvature thresholds were experimentally tested. We chose the following thresholds: $H_i = \pm 0,05$, $K_i = \pm 0,0005$ of median and Gaussian curvatures, respectively. After converting curvatures that satisfy $-0,05 < H < 0,05$ and $0,0005 < K < 0,0005$ to zero, the same regions appears isolated in most of faces as shown in Figure 2(d). Segmentation became simpler and easier because the region candidate number per each region were reduced to one in most cases. Regions and lines to be segmented (from which the facial features to represent the individuals in a face recognition system, will be obtained) are shown in Figure 3. The region selection criteria is: to select those regions of pronounced curvature, whose shape has low dependence when facial expressions appear.

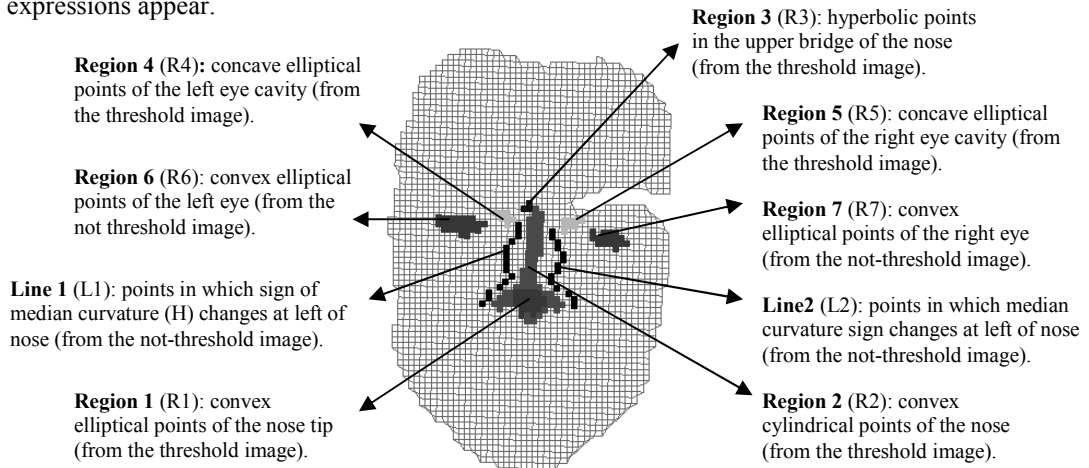


Fig 3. Segmented regions of a face from which facial features are extracted. Regions number 6 and 7 are from non-threshold image shown in Figure 2 (c). Lines 1 and 2 can be observed in the non-threshold image shown in Figure 2 (a).

The methodology employed for automatic segmentation of the selected regions is as follows. Region 1 is easily distinguishable because is the region which has the highest number of convex elliptic nodes in the threshold image. Region 2 is formed by the convex cylindrical points and it is neighbour of region 1. Points of Region 3 are hyperbolic ones and located in a neighbour region of the Region 2 which is up from it. Further relative position restrictions with respect to the eye regions can be used if more than one candidate region were obtained. Regions 4 and 5 are formed by concave elliptic points. There are few candidate regions to them, and the selection is performed according to their relative position with respect to the nose regions. Regions 6 and 7 are formed by convex elliptic points in the non-threshold image, eliminating candidate regions that did not followed certain restrictions. Such restrictions were: their relative positions with respect to regions 3, 4 and 5 (for example, their points had to be found in a band containing these three regions), height (1.7 mm. maximum) and width of the candidate regions. Lines 1 and 2 are looked for from the external border of Region 2 (compressed between the centroids of the regions 4 and 5 and the centroid of the region 1) at left and right directions respectively until a sign change of the median curvature is found.

A region or line location result can be labelled as: a) failure (F in Table 1), b) non-existence (NE in Table 1) and c) correct location (C in Table 1). Failure means that a searched region or line was found in a bad location and then, a false positive in the region location was found as the chosen region. Non-existence means that there was not any region resulting for the searched region. Correct location occurs when the segmented region was correctly found. Failure, Non existence and correct percentage results for the different regions and views in the whole database after the segmentation are shown in Table 1.

		Region 1	Region 2	Region 3	Region 4	Region 5	Region 6	Region 7	Line 1	Line 2
looking down	F	0%	0%	0%	0%	0%	8,3%	6,6%	0%	0,6%
	NE	0%	0%	1,2%	15%	15%	28,3%	51,6%	0%	0%
	C	100%	100%	98,8%	90%	90%	63,4%	41,8%	100%	99,4%
looking up	F	0,6%	0,6%	1,2%	0,6%	0,6%	1,2%	0,6%	0,6%	0,6%
	NE	0%	0%	18,3%	6,6%	8,3%	8,3%	15%	0%	1,2%
	C	99,4%	99,4%	80,5%	92,8%	91,1%	90,5%	84,4%	99,4%	98,2%
frontal view	F	0%	0%	0,6%	0%	0%	0,6%	0%	0%	0%
	NE	0%	0%	6,6%	5%	1,2%	6,6%	1,2%	0%	0%
	C	100%	100%	92,8%	95%	98,8%	92,8%	98,8%	100%	100%
frontal view	F	0%	0%	0,6%	0%	0%	0,6%	0,6%	0%	0%
	NE	0%	0%	5%	8,3%	5%	6,6%	5%	0%	0%
	C	100%	100%	94,4%	91,7%	95%	92,8%	94,4%	100%	100%
random gesture	F	0%	0%	0%	0%	0%	0,6%	0,6%	0%	0%
	NE	0%	0%	8,3%	0,6%	1,2%	5%	10%	0%	0%
	C	100%	100%	91,7%	99,4%	98,8%	94,4%	89,4%	100%	100%
laugh	F	0%	0%	0%	0%	0%	1,2%	0,6%	5%	1,2%
	NE	0%	0%	6,6%	0,6%	1,2%	5%	10%	0%	0%
	C	100%	100%	93,4%	99,4%	98,8%	93,8%	89,4%	95%	98,8%
smile	F	0%	0%	0%	0%	0%	0%	0%	0,6%	0%
	NE	0%	0%	6,6%	0,6%	0,6%	6,6%	6,6%	0%	0%
	C	100%	100%	93,4%	99,4%	99,4%	93,4%	93,4%	99,4%	100%
Total views	F	0,2%	0,2%	0,95%	0,2%	0,2%	2,85%	1,9%	1,19%	0,95%
	NE	0%	0%	7,85%	5,71%	5,71%	9,5%	14,5%	0%	0,2%
	C	99,8%	99,8%	91,2%	94,09%	94,09%	87,65%	83,6%	98,81%	98,85%

Table 1. Failure (F), non-existence (NE) and correct location (C) percentages obtained in the region and line location stage. Results are grouped per searched regions and lines over each set of 60 images corresponding to each kind of view. Last rows are the percentages per searched regions and lines over the 420 images of the database.

The poorest segmentation results were obtained in the eye region location, in particular, when the view of the individuals presented light rotation when the individual was looking down. Occluded eye regions were automatically reconstructed by the software of the 3D digitizer using an interpolation algorithm. This produced a pernicious effect in the surface, smoothing it and losing information of the real curvature. This phenomena also occurred in the region 3 location placed around the nasion point when individuals were looking up. Nose point region (Region 1) offers better results than the other regions, failing only when the image has a hole of the surface in this place. A failure of this region location produces failures in the rest of region locations, cause of this regions are looked for in relative positions to it. While a failure (F in Table 1) on a region searching produces a recognition error, a non existence (NE in Table 1) of some region makes possible the face recognition stage.

5 Feature extraction

After the segmentation task, a feature extraction stage is performed. Eighty six non-independent features extracted from the segmented regions were computed. Table 2 describes and classifies these features into categories (areas, distances, angles, curvature average of a region, etc.). Each feature has an associated identification number and a ranking position. This position corresponds to the ordered discriminating power of the feature in such a way that features presenting high discriminating power have a small rank position and

those presenting less discriminating power have a large rank position. Discriminating power estimation of each feature Φ has been computed using the Fisher coefficient [4], which represents the ratio of between-class variance to within-class variance, according to the formula

$$\frac{\sum_{i=1}^c (m_i - m)^2}{\sum_{i=1}^c \frac{1}{n_i} \sum_{x \in \Phi_i} (x - m_i)^2} \quad (3)$$

were c is the number of classes or subjects, Φ_i is the set of feature values for class i , n_i is the size of Φ_i , m_i is the mean of Φ_i , and m is the global mean of the feature over all classes. There are 60 classes corresponding to the number of distinct subjects. Although there are seven images per person, when computing the Fisher coefficients, only the 3D facial images having the whole regions and consequently the whole features correctly extracted have been employed.

When a feature can not be computed (always be cause of the non-existence of the region/s from which it is derived), it is zero valued, except when a symmetric feature exists (then, the non-existent feature is valued like its symmetric feature). Furthermore, area based features result to be zero valued when there are less than three points belonging to the quadrilaterals forming such regions. Extracted features have been normalised to values in the rank from 0 to 1. Figure 4 relates the Fisher coefficients corresponding to each feature rank position in the Fisher coefficient ordered list.

id. num	feature description	rank pos.	id. num	feature description	rank pos.
Area of the regions			Mean H of the points belonging to a region		
0	A R1	52	40	H R1	28
1	A R4	41	41	H R2	24
2	A R5	47	42	H R3	16
3	A R2	30	43	H R4	17
4	A R3	35	44	H R5	21
5	A R6	45	45	H (R4 U R5)	12
6	A R7	50	46	H R6	53
Area relations			47	H R7	63
7	A R2/A R1	59	48	H (R6 U R7)	48
8	A R1/A R3	71	Mean K region of the points belonging to a region		
9	A R1/(A R4+A R5)	70	49	K R1	33
10	A R1/(A R6+A R7)	58	50	K R2	37
Mean of areas			51	K R3	11
11	(A R4 + A R5)/2	38	52	K R4	20
12	(A R6+A R7)/2	42	53	K R5	22
Distance between mass centres of regions			54	K (R4 U R5)	13
13	d(C R4, C R5)	18	55	K R6	55
14	d(C R6, C R7)	81	56	K R7	64
15	d(C R1, C R3)	6	57	K (R6 U R7)	51
16	d(C R4, C R3)	8	Variance H region of the points belonging to a region		
17	d(C R5, C R3)	9	58	VH R1	74
18	d(C R6, C R3)	36	59	VH R2	85
19	d(C R7, C R3)	34	60	VH R3	62
20	d(C R6, C R1)	61	61	VH R4	83
21	d(C R7, C R1)	60	62	VH R5	72
22	d(C R4, C R1)	15	63	VH (R4 U R5)	68
23	d(C R5, C R1)	19	64	VH R6	79
Relations among distances between mass centres of regions			65	VH R7	86
24	d(C R4, C R5)/d(C R1, C R3)	10	66	VH (R6 U R7)	78
25	1/2[d(C R4, C R3)+d(C R5, C R3)]/d(C R3, C R1)	32	Variance K region of the points belonging to a region		
26	d(C R6, C R7)/d(C R3, C R1)	49	67	VK R1	73
27	1/2[d(C R6, C R3)+d(C R7, C R3)]/d(C R3, C R1)	40	68	VK R2	69
Mean distance			69	VK R3	82
28	1/2[d(C R4, C R3)+d(C R5, C R3)]	5	70	VK R4	77
29	1/2[d(C R6, C R3)+d(C R7, C R3)]	29	71	VK R5	67
76	1/2[d(C R6, C R1)+d(C R7, C R1)]	57	72	VK (R4 U R5)	66
77	1/2[d(C R4, C R1)+d(C R5, C R1)]	14	73	VK R6	75
Angles among mass centres of regions			74	VK R7	84
30	ang(C R4, C R3, C R5)	1	75	VK (R6 U R7)	80
31	ang(C R4, C R3, C R1)	2	Lines 1 and 2 based features		
32	ang(C R5, C R3, C R1)	4	78	d(upper end point L1, upper end point L2)	43
33	ang(C R4, C R1, C R5)	31	79	d(lower end point L1, lower end point L2)	65
34	ang(C R6, C R1, C R7)	76	80	Lenght of L1	44
35	ang(C R6, C R3, C R7)	27	81	Lenght of L2	46
36	ang(C R6, C R3, C R1)	23	82	1/2 [Lenght of L1 + Lenght of L2]	39
37	ang(C R7, C R3, C R1)	26	83	Area of the polygon formed by the 4 ends of L1,L2	54
Mean angle			84	ang(lower point of L1,C R1, lower end of L2)	56
38	1/2[ang(C R4,C R3,C R1)+ang(C R5, C R3,C R1)]	3	85	ang(upper point of L1,C R3, upper end of L2)	7
39	1/2[ang(C R6,C R3,C R1)+ang(C R7, C R3,C R1)]	25			

Table 2. Extracted features from the segmented regions and lines, and their position in an ordered list according to their discriminating power. The used acronyms are: R_i = region i ; L_i = line i ; A_{Ri} = area of region i ; C_{Ri} = centroid of region i ; $d(P1, P2)$ = Euclidean distance between 3D points $P1$ and $P2$; $ang(P1, P2, P3)$ = angle defined by the 3D points $P1, P2$ and $P3$, being $P2$ the intermediate vertex; H_{Ri} and K_{Ri} are the respective averages of the mean and Gaussian curvatures, evaluated in points belonging to the region i ; VH_{Ri} and VK_{Ri} are the respective variances of the mean and Gaussian curvatures evaluated in points belonging to the region i .

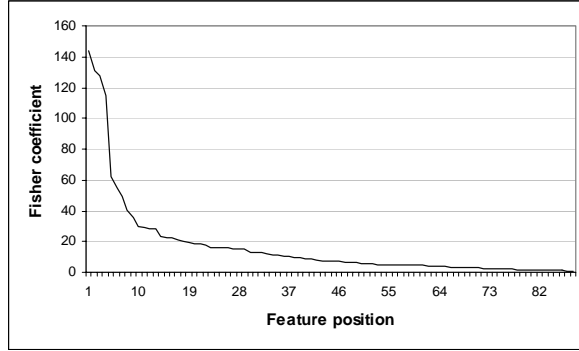


Figure 4. Fisher coefficient values corresponding to each feature rank position in the ordered list according to the Fisher coefficients.

6 Feature selection

Like in many other pattern recognition applications, a reduction of the number of features is needed to increase the efficiency of the face recogniser. In order to select an optimal feature subset to represent individuals for face recognition purposes, eighty six features subsets were tested: those using the first n features in the ordered list for all n , such as $1 \leq n \leq 86$. The set of known faces of the face recognition system (training set) consisted in 60 frontal images (one per individual) selected such that they present the whole existing regions and the whole features successfully computed. Six test sets were used separately: rotated looking down image set, rotated looking up image set, the other frontal image set (different from the train set) without facial expressions, the random gesture set, the laugh gesture set, and the smile set. The matching procedure was based on the minimum Euclidean distance classifier. Test sets presenting the existence of the whole regions consisted of 19, 41, 50, 47, 45 and 48 images, respectively. Among these six test sets, best recognition results were obtained when the feature number used to represent the individuals was ranked between the first 33 and 37 features (those of lower positions in the ordered list according to Fisher coefficients). It can be appreciated in the Figure 5 which shows the recognition percentages corresponding to different numbers of considered features, when only images presenting existence of the whole regions are used. For this reason, the feature subset formed by the first 35 ranked features has been selected to represent faces in our face recognition system experiments. Figure 5 (a) shows the recognition success percentage when the test set was the frontal image set and (b) when the test set was the smile set. Each curve in Figure 5 represents the recognition success percentage obtained when test individuals are found in one, two, three, five and eight nearest (in terms of Euclidean distance) selected train images, respectively. Only images presenting whole regions have been tested for the feature selection purpose.

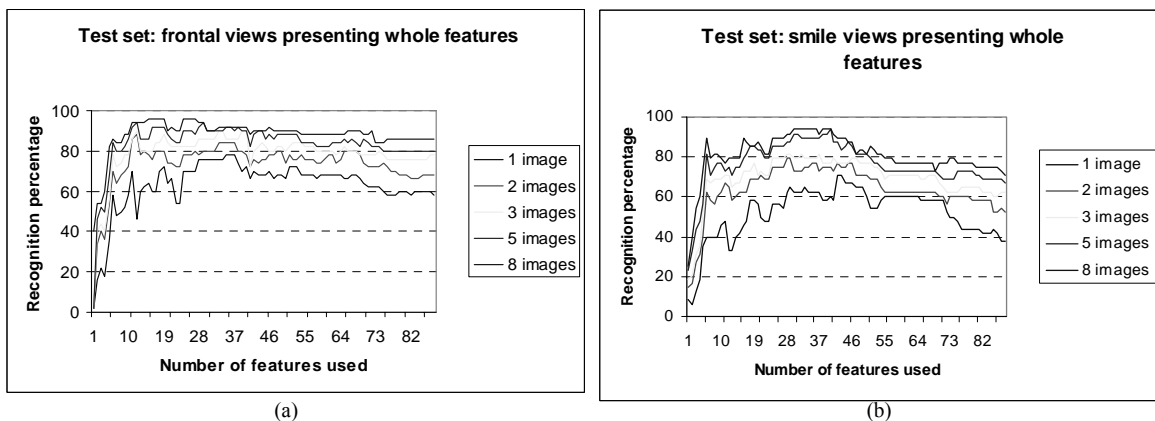


Figure 5. Recognition rates corresponding to each feature subset with highest n Fisher coefficients ($1 \leq n \leq 86$). (a) Test set is formed by frontal views and (b) by smile views, containing the whole regions and features correctly extracted.

7 Face recognition experiments

After the feature discriminating power analysis, the first 35 features of the ordered list of features according to the Fisher coefficients were used to represent faces in our face recognition experiments. The aim of these

experiments was searching the feature vector belonging to the training set whose Euclidean distance to each test set image was minimal. Training set of known faces was formed by 60 frontal images of the 60 individuals with existence of whole regions and consequently features. Six test sets were used separately, each one of them formed by the set of not used images belonging to one of the 6 different views available: looking down, looking up, frontal without facial expression and three frontal sets presenting facial expressions (random gesture, laugh and smile). Two different experiments were performed. First, we tested sets formed only by faces in which all regions existed, and consequently, all features could be computed. In a second experiment, all images of the 60 individuals contained in each set of test images were tested, presenting or not all features. In the second experiment, when a feature could not be computed it had an associated zero value, and it was not used in the Euclidean distance formulae.

Recognition success rates of both experiments are presented in Figure 6. Best results were obtained when only images containing all features were tested, although the reduction of the recognition rate testing all images is around 5%. Another aspect to mention relative to the second experiment is that when feature vectors are 35 feature long, all test images could be matched because some of these 35 features were present. Figure 7 shows the number of test images that could be matched (cause of the existence of sufficient extracted features to be used) per feature number to be used as feature vector components.

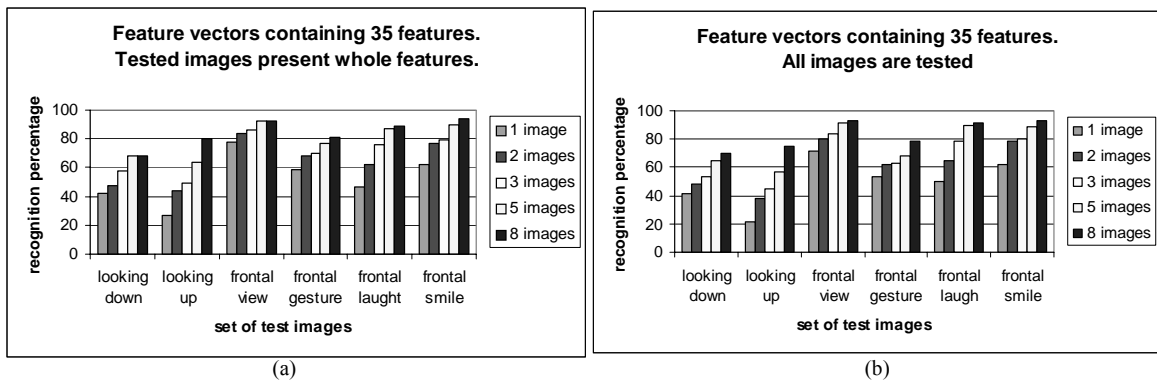


Figure 6. Experimental results of the face recognition success percentage per set of test images using the first 35 more discriminating features to represent faces (a) testing images containing the whole features and (b) testing images with the possibility of that not all features were present and have been correctly located.

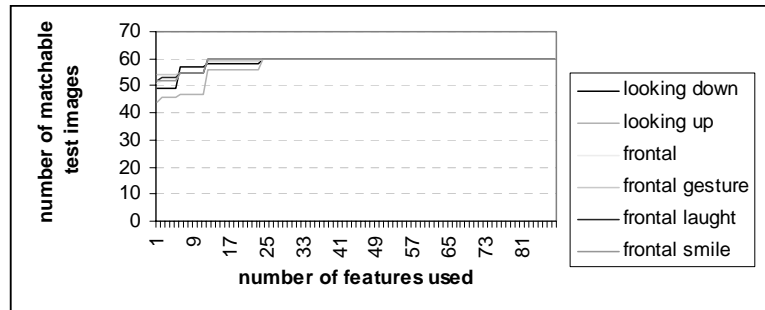


Figure 7. Number of test images having some feature of the selected features to be used in the match, in the second group of test experiments.

8 Conclusions and future work

A database of 420 3D facial images with 60 individuals was acquired for training and testing the face recognition system. Among these images, 310 of them presented all regions and lines correctly segmented, and the corresponding extracted features were also correct; 20 images presented one or more false positives in their region location and these images were badly represented by means of non-correct features; and in 90 images not all the regions existed but the obtained features from the existing regions were correctly computed and they were able to represent faces to be used in the face recognition system (due to length of the feature vectors could be variable). The features offering better recognition results were angles and distances measured using centroids of regions as well as averages of mean and Gaussian curvatures of regions. Area based features offered poorest discriminating power, due to their corresponding larger variation in within-class variance of the feature according to Fisher's criterion. This may be due to the fact that the segmented regions are very small, containing scarce number of points, and small variations in the number of points can produce significant differences among areas of a region in within-class individuals. Curvature variances evaluated for each region resulted in having low discriminating power in the selected regions. After the

analysis of the discriminating power of 66 3D facial features in the experiments of face recognition using different subsets of features, better recognition ratios were obtained when the 35 more discriminating features were used to represent faces. Best recognition results using the 35 more discriminating features were obtained when frontal views were tested (78%, 84%, 86%, 92%, 92% of success when respectively the first one, two, three, five and eight matches were selected). The second best recognition results were obtained using views containing smile expressions (62%, 77,08%, 79,17%, 89,58% and 93% of success when respectively the first one, two, three, five and eight matches were selected), and other gesture images. The worst recognition results were obtained when the test sets consisted in rotated faces around x axis. These results were obtained when only images presenting the whole features were tested. When all test images were used, presenting or not all regions (and correctly located or not), a small deterioration of the recognition percentages were obtained (for example, in frontal images 71,67%, 80%, 83,33%, 91,67% and 93,3% of success when respectively the first one, two, three, five and eight matches were selected). This was compensated by the fact that a higher number of images can be tested including those images in which not all the regions and consequently features were present. Another conclusion is that it would be better to omit the x -rotated views (those where the individual is looking up and looking down) in the task of computing the Fisher coefficients, because they can introduce some errors due to occlusions.

As future work, it would be convenient to choose other features different from those belonging to the eye regions when faces are rotated looking up and looking down because their corresponding regions appear occluded in many patterns. Also, to develop a validation procedure to reject false positives in the region location is a critical task to improve the obtained results. A failure in a region or line location is easily detectable because, usually the chosen candidate region is very far from the correct location, and the size of the wrong region candidate differs a lot from the correct size of the searched region.

References

- [1] Y. Aoki y S. Hashimoto (1998). Physical Facial Model Based on 3D-CT Data for Facial Image Analysis and Synthesis, *Proc. Second Intl. Conf. on Automatic Face and Gesture Recognition*, IEEE Comp. Society, Nara (Japan): 448-453.
- [2] R. J. Campbell and P. J. Flynn (2001). A Survey of Free-Form Object Representation and Recognition Techniques, *Computer Vision and Image Understanding*, 81: 166-210.
- [3] A.M. Haider and T. Kaneko (2001). Automated 3D-2D Projective Registration of Human Facial Images using Edge Features, *International Journal of Pattern Recognition and Artificial Intelligence*, 15(8): 1263-1276.
- [4] P. Hallinan, G. G. Gordon, A. L. Yuille, P. Giblin and D. Mumford (1999). *Two and Three-dimensional patterns of the face*, Ed. A. K. Peters.
- [5] Horace H. S. Ip, Lijun Yin, (1996). Constructing a 3D individualized head model from two orthogonal views, *The Visual Computer*, 12, Springer-Verlag: 254-266
- [6] T. Huang and L. Tang (1995). 3D Model-based Video Coding: Computer Vision meets Computer Graphics, *International Computer Science Conference*.
- [7] T. S. Huang and Li-an Tang (1996). 3-D Face Modelling and its Applications, *International Journal of Pattern Recognition and Artificial Intelligence*, 10, No. 5.
- [8] A. López de la Rica, A. de la Villa Cuenca (1997). Geometría Diferencial, Ed. CLAGSA.
- [9] <http://www.minolta3d.com/index.asp>
- [10] S. Pankanti, R.M. Bolle, A. Jain (2000). Biometrics: The Future of Identification, *IEEE Computer*: 46-49.
- [11] A.Pentland, T.Choudhury (2000). Face Recognition for Smart Environments, *IEEE Computer*: 50-55.
- [12] P.J. Phillips, P.J., Wechsler, H., Huang J.S., and Rauss, P.J. (1998). The FERET Database and Evaluation Procedure for Face-Recognition Algorithms, *Image and Vision Computing*, 16(5): 295-306.
- [13] P. J. Phillips, A. Martin, C. L. Wilson y Mrk Przybocki (2000). An Introduction to Evaluating Biometric Systems, *IEEE Computer*: 56-64.
- [14] E. Trucco and A. Verri (1998). *Introductory Techniques for 3-D Computer Vision*, Prentice-Hall.
- [15] Mun Way Lee and Surendra Ranganath (2003). Pose-invariant face recognition using a 3D deformable model, *Pattern Recognition* 36: 1835-1846.